

**DEFECTIVE PARTICLE SURFACE ON ZnO AND  
ITS INFLUENCE ON THE OPTICAL,  
ELECTRONIC AND TOXICITY PROPERTIES**

**NUR MARIAM BINTI KAMARUDDIN**

**UNIVERSITI SAINS MALAYSIA**

**2023**

**DEFECTIVE PARTICLE SURFACE ON ZnO AND  
ITS INFLUENCE ON THE OPTICAL,  
ELECTRONIC AND TOXICITY PROPERTIES**

by

**NUR MARIAM BINTI KAMARUDDIN**

**Thesis submitted in fulfilment of the requirements  
for the degree of  
Doctor of Philosophy**

**July 2023**

## ACKNOWLEDGEMENT

Alhamdulillah. All praises to Allah who gave me the strength, endurance, and ability to pursue and complete this research. I appreciate and would like to express my deepest gratitude to my main supervisor Professor Madya Dr. Shahrom Mahmud for his guide and tutor in the whole research work. I also would like to thank my co-supervisor Professor Madya Dr. Azman Seenii for the help, guide, and support in providing and sharing the research facility at Institute Penyelidikan Pergigian Termaju, (IPPT) Bertam for me to conduct the experiment. I would like to extend my gratitude to all the lab assistance of the Institute of Nano-optoelectronic research (INOR) in the School of Physics for their valuable contributions and for sharing the knowledge. I am thankful to my sponsor, the Malaysian Ministry of Higher Education (MyBrain15), for providing the scholarship and adequate funding to allow me to continue my PhD studies. In addition, my special appreciation also goes to my husband, Ahmad Afiq Sabqi, and my children, Ahmad Anas Syazwan and Aileen Sofea for their encouraged and patience during my PhD journey. Finally, special thanks to my parents, Kamaruddin Ibrahim and Salimah Sar who always support and help me in finishing my studies.

Thank you so much.

Nur Mariam Kamaruddin

## TABLE OF CONTENTS

<b>ACKNOWLEDGEMENT.....</b>	<b>ii</b>
<b>TABLE OF CONTENTS.....</b>	<b>iii</b>
<b>LIST OF TABLES.....</b>	<b>vii</b>
<b>LIST OF FIGURES.....</b>	<b>viii</b>
<b>LIST OF EQUATION.....</b>	<b>xiii</b>
<b>LIST OF ABBREVIATION.....</b>	<b>xiv</b>
<b>LIST OF SYMBOLS.....</b>	<b>xvi</b>
<b>ABSTRAK.....</b>	<b>xviii</b>
<b>ABSTRACT.....</b>	<b>xx</b>
<b>CHAPTER 1 INTRODUCTION .....</b>	<b>1</b>
1.1 Background of Study.....	1
1.2 Problem Statement.....	3
1.3 Objectives of Study.....	5
1.4 Scope of Study.....	5
1.5 Thesis Outline.....	6
<b>CHAPTER 2 LITERATURE REVIEW.....</b>	<b>8</b>
2.1 Introduction.....	8
2.2 Nanomaterial.....	8
2.3 ZnO Powder.....	10
2.4 Application of ZnO.....	11
2.5 Properties of ZnO.....	14
2.6 Electrical Properties of ZnO.....	16

2.7	Optical Properties of ZnO.....	17
2.7.1	Non-radiative via Deep Level Energy.....	19
2.7.2	Auger Recombination.....	20
2.7.3	Surface Recombination.....	21
2.8	Surface Modification of ZnO by Annealing.....	22
2.9	Toxicity of ZnO.....	24
2.10	Fibroblast Cell Lines.....	25
2.11	Breast Cancer.....	26
2.12	Anti-cancer Activity on ZnO.....	28
2.13	Reactive Oxygen Species.....	32
2.14	Mechanisms of ZnO Toxicity .....	34
	<b>CHAPTER 3 METHODOLOGY .....</b>	<b>38</b>
3.1	Introduction.....	38
3.2	Design of Experiment.....	38
3.3	Annealing Treatment.....	40
3.4	Characterization of ZnO.....	41
3.4.1	Electron Microscopy .....	41
3.4.1(a)	Electron Spectroscopy Imaging (ESI).....	42
3.4.1(b)	Transmission Electron Microscopy (TEM).....	43
3.4.1(c)	Field Emission Scanning Electron.....	45
	Microscopy (FESEM)	
3.4.2	Current-Voltage Measurement.....	47
3.4.3	X-ray Diffraction (XRD).....	48
3.4.4	UV-Visible Spectroscopy.....	51

3.4.5	Raman Spectroscopy .....	53
3.4.6	Photoluminescence (PL) .....	57
3.5	Cell Culture.....	60
3.6	Cell Cultures Properties.....	61
3.6.1	Reagents.....	61
3.6.2	Commercial Kits.....	62
3.6.3	Laboratory apparatus, equipment, and consumables.....	62
3.7	L929 Cells.....	62
3.7.1	Cytotoxicity Testing of ZnO on L929 Cells.....	63
3.8	Michigan Cancer Foundation-7 (MCF-7) Cells.....	65
3.8.1	Determination of Half Maximal Inhibitory Concentration (IC <sub>50</sub> ) .....	65
3.8.2	Cell Proliferation Assay.....	67
3.9	Microscopy Observation of Morphological Changes.....	67
<b>CHAPTER 4 RESULTS AND DISCUSSION.....</b>		<b>69</b>
4.1	Introduction.....	69
4.2	Transmission Electron Microscopy (TEM)-Electron Spectroscopy .....	69
	Imaging (ESI) Analysis	
4.3	Field Emission Scanning Electron Microscopy (FESEM) Analysis.....	74
4.4	Current-Voltage Analysis.....	80
4.5	X-ray Diffraction (XRD) Analysis.....	84
4.6	UV-Visible Analysis .....	88
4.7	Raman Spectroscopy Analysis .....	91
4.8	Photoluminescence (PL) Analysis .....	92
4.9	Cytotoxicity Effect of ZnO on L929 Cells.....	96

4.10	Half Maximal Inhibitory Concentration (IC <sub>50</sub> ) Result.....	103
4.11	Proliferation Effect of ZnO.....	109
4.12	Key Factor of Anticancer Activity.....	112
4.13	Proposed Mechanisms of Anticancer Activity.....	114
4.13.1	Reactive Oxygen Species (ROS) Generation.....	115
4.13.2	Zinc Ions (Zn <sup>2+</sup> ) Release.....	117
	<b>CHAPTER 5 CONCLUSION.....</b>	<b>119</b>
5.1	Conclusion.....	119
5.2	Future Perspectives.....	121
	<b>REFERENCES.....</b>	<b>123</b>
	<b>APPENDICES</b>	
	<b>LIST OF PUBLICATIONS</b>	

## LIST OF TABLES

	<b>Page</b>
Table 2.1	Typical properties of ZnO.....15
Table 4.1	Structural parameters of ZnO-AG; ZnO-O <sub>2</sub> ; ZnO-N <sub>2</sub> .....86
Table 4.2	Raman shift of ZnO-AG; ZnO-O <sub>2</sub> ; ZnO-N <sub>2</sub> .....92
Table 4.3	Cell viability and differences between growth suppression of.....112 ZnO-O <sub>2</sub> and ZnO-N <sub>2</sub> without changing the medium.
Table 4.4	Cell viability and differences between growth suppression of.....112 ZnO-O <sub>2</sub> and ZnO-N <sub>2</sub> with medium changes on day 5 and day 7.



## LIST OF FIGURES

	<b>Page</b>
Figure 2.1	11
Shape of ZnO (a) five different nanostructures.....11 (microbox, nanorod, nanoplate, polyhedron, ISP) (b) microclusters, (c) irregularly shaped particles (ISP) (d) hexagonal drum, (e) microrod, (f) hexagonal heads of nanorod, (g) nanomallet, (h) microbox, (i) family of nanoplates, (j) long rectangular nanoplates	
Figure 2.2	12
Application of ZnO .....	
Figure 2.3	15
Hexagonal wurtzite-type lattice of ZnO crystal structure.....	
Figure 2.4	18
(a) Radiative recombination (b) non-radiative recombination.....	
Figure 2.5	19
Band transitions in a semiconductor (a) non-radiative via deep.....19 level (b) non-radiative via Auger process (c) radiative with a photo emission.	
Figure 2.6	20
Energy levels of native defects in ZnO.....	
Figure 2.7	21
The Auger recombination process.....	
Figure 2.8	22
Fermi level is pinned by the overall charge state at the.....22 surface (a)formation energies of the O vacancy ( $V_O$ ) (b) formation energies of ( $V_O$ ) the Zn interstitial ( $Zn_i$ ), the Zn antisite ( $Zn_O$ ), and the Zn vacancy ( $V_{Zn}$ )	
Figure 2.9	27
Distribution of cases and deaths for the Top 10 most common.....27 cancers in 2020 for both sexes	
Figure 2.10	28
Normal and cancer cells.....	
Figure 2.11	29
Schematic diagram of factors influence toxicity of ZnO.....	

Figure 2.12	The toxicity of ZnO against human cervical carcinoma cells.....	30
Figure 2.13	Electron structures of common reactive oxygen species.....	32
	Each structure is provided with its name and chemical formula.	
	The red dots designate an unpaired electron	
Figure 2.14	Schematic diagram of a proposed toxicity mechanism.....	35
Figure 3.1	Schematic design of experiment.....	39
Figure 3.2	ZnO powder .....	40
Figure 3.3	Annealing tube furnace LENTON VTF/12/60/700.....	41
Figure 3.4	Interactions and secondary effects of electron beam-specimen.....	42
Figure 3.5	EFTEM Zeiss Libra 120.....	43
Figure 3.6	TEM Philips CM12.....	44
Figure 3.7	FESEM Nova Nano SEM 450 FEI.....	46
Figure 3.8	Current-voltage Keithley model 4200-SCS.....	47
Figure 3.9	X-ray diffraction on crystalline lattice.....	50
Figure 3.10	PANalytical X' pert PRO MRD Pw3040 X-ray diffractometer.....	51
Figure 3.11	UV-Vis Cary 5000 spectrophotometer.....	52
Figure 3.12	Instrumentation of UV-Visible.....	52
Figure 3.13	Diagram of the Rayleigh and Raman scattering processes.....	55
Figure 3.14	PL Raman Horiba Jobin-Yvon HR-800 UV.....	56
Figure 3.15	Schematic diagrams of PL setup.....	57
Figure 3.16	Recombination process in a semiconductor.....	59
	(a) Band-to-band recombination. (b) Band-to-acceptor transition.	

(c) Donor-to-valence transition. (d) Donor-to-acceptor-pair transition. (e) Recombination via a deep center. (f) Nonradiative recombination via an intermediate state. (g) Band-to-band Auger recombination

Figure 3.17	Haemocytometer chamber .....	61
Figure 3.18	Count of Cells.....	64
Figure 3.19	Olympus Xcam Alpha camera.....	68
Figure 4.1(a)	EFTEM-ESI mapping of ZnO-AG.....	71
Figure 4.1(b)	EFTEM-ESI mapping of ZnO-O <sub>2</sub> .....	72
Figure 4.1(c)	EFTEM-ESI mapping of ZnO-N <sub>2</sub> .....	73
Figure 4.2	TEM images of (a) ZnO-AG (b) ZnO-O <sub>2</sub> (c) ZnO-N <sub>2</sub> .....	74
Figure 4.3	FESEM micrographs of (a) ZnO-AG; (b) ZnO-O <sub>2</sub> ; (c) ZnO-N <sub>2</sub> .....	75
Figure 4.4(a)	The average particle sizes of ZnO-AG.....	76
Figure 4.4(b)	The average particle sizes of ZnO-O <sub>2</sub> .....	77
Figure 4.4(c)	The average particle sizes of ZnO-N <sub>2</sub> .....	77
Figure 4.5	The EDS analysis for (a) ZnO-AG (b) ZnO-O <sub>2</sub> (c) ZnO-N <sub>2</sub> .....	79
Figure 4.6	The atomic % of (O:Zn) in (a) ZnO-AG (b) ZnO-O <sub>2</sub> (c) ZnO-N <sub>2</sub> .....	80
Figure 4.7	Current–Voltage Measurement of ZnO.....	82
Figure 4.8	Schematic diagram of the surface band bending of ZnO at.....	83
	two different stages (a) ZnO-O <sub>2</sub> (b) ZnO-N <sub>2</sub>	
Figure 4.9	XRD spectra of ZnO-AG; ZnO-O <sub>2</sub> ; ZnO-N <sub>2</sub> .....	85
Figure 4.10	Optical absorption spectra of (a) ZnO-AG (b) ZnO-O <sub>2</sub> (c) ZnO-N <sub>2</sub> ...	90

Figure 4.11	Raman spectra of ZnO-AG; ZnO-O <sub>2</sub> ; ZnON <sub>2</sub> .....	91
Figure 4.12	Photoluminescence spectra of ZnO-AG; ZnO-O <sub>2</sub> ; ZnO-N <sub>2</sub> .....	93
Figure 4.13	Schematics of the energy band diagram for.....	96
	(a) ZnO-O <sub>2</sub> (b) ZnO-N <sub>2</sub>	
Figure 4.14	Schematic diagram for Reliablue Assay procedure.....	98
Figure 4.15	Percentage of viable cells L929 after 72h treatment.....	99
	with different concentration of ZnO sample.	
	Mean ± SD (n = 3). (ANOVA) followed by	
	Bonferroni correction indicated statistically significant	
	difference when compared with control (*P ≤ 0.05)	
Figure 4.16	Light microscopic images of L929 cell lines.....	102
	under treatment of: (a) negative control.	
	(b) 0.3125 mM ZnO sample (c) 0.5 mM ZnO sample.	
Figure 4.17	Percentage of inhibitory concentration (IC <sub>50</sub> ) of.....	104
	ZnO nanoparticles treated MCF-7 cells: (a) ZnO-AG	
	(b) ZnO-O <sub>2</sub> (c) ZnO-N <sub>2</sub> . Mean ± SD (n = 3). (ANOVA)	
	followed by Bonferroni correction indicated statistically	
	significant difference when compared with control (*P ≤ 0.05)	
Figure 4.18	Morphological changes of treated cells at IC <sub>50</sub> and.....	107
	0.25mM for (a) ZnO-AG (b) ZnO-O <sub>2</sub> (c) ZnO-N <sub>2</sub>	
Figure 4.19	The proliferative rate of MCF-7 cells via cell viability.....	110
	of treated cells with ZnO samples and untreated cells	
	for seven days using MTT assay without changing the	
	medium. Mean ± SD (n = 3). (ANOVA) followed by Bonferroni	
	correction indicated statistically significant difference	
	when compared with control (*P ≤ 0.05)	
Figure 4.20	The proliferative rate of MCF-7 cells via cell viability.....	111

of treated cells with ZnO samples and untreated cells for seven days using MTT assay with medium changing on day 5 and day 7. Mean  $\pm$  SD (n = 3). (ANOVA) followed by Bonferroni correction indicated statistically significant difference when compared with control (\*P  $\leq$  0.05)

Figure 4.21 Proposed mechanism of toxicity towards MCF-7 cells.....115

## LIST OF EQUATION

	<b>Page</b>
Equation 2.1 Recombination rate of surplus carriers.....	21
Equation 3.1 Photon energy.....	48
Equation 3.2 Bragg's law.....	49
Equation 3.3 Beer - Lambert law.....	53
Equation 3.4 Absorbance .....	53
Equation 3.5 Cell concentration.....	64
Equation 3.6 Simplified cell concentration.....	64
Equation 4.1 Electrical resistance.....	80
Equation 4.2 Scherer's formula.....	85
Equation 4.3 Braggs equation.....	86
Equation 4.4 Lattice equation.....	87
Equation 4.5 Strain equation.....	87
Equation 4.6 Stress equation.....	88
Equation 4.7 Energy band gap equation.....	89
Equation 4.8 Cell viability for Reliablue assay.....	99
Equation 4.9 Cell viability for MTT assay .....	105

## LIST OF ABBREVIATIONS

$E_c$	Conduction band
EDS	Energy dispersive spectroscopy
EFTEM	Energy-filtering transmission electron microscope
ESI	Electron spectroscopy imaging
$E_v$	Valence band
FESEM	Field-emission scanning electron microscope
FWHM	Full width half maximum
GL	Green luminescence
IC <sub>50</sub>	Half maximal inhibitory concentration
I-V	Current voltage
L929	Mouse skin fibroblast cell line
MCF-7	Breast cancer cell
NBE	Near-band-edge
O	Oxygen
PL	Photoluminescence
ROS	Reactive oxygen species
SD	Standard deviation
TEM	Transmission electron microscope
UV	Ultraviolet
UVA	Ultraviolet-A
$V_o$	Oxygen vacancy
XRD	X-ray diffraction
Zn	Zinc

Zn <sub>i</sub>	Zinc interstitial
ZnO	Zinc oxide
ZnO-AG	Zinc oxide as grown
ZnO-O <sub>2</sub>	Zinc oxide annealed oxygen
ZnO-N <sub>2</sub>	Zinc oxide annealed nitrogen



## LIST OF SYMBOLS

$a$	Basal plane lattice constant
$c$	Uniaxial lattice constant
$u$	Internal coordinate
$hkl$	Miller indices
$T$	Absolute temperature
$C_p$	Specific heat capacity
$\omega$	Phonon frequency
$R_s$	Recombination rate
$\tau$	Lifetime
$O_2^-$	Superoxide anion
$H_2O_2$	Hydrogen peroxide
$\cdot OH$	Hydroxyl radical
$E$	Energy
$h$	Planck's constant
$c$	Speed of light
$\lambda$	Wavelength
$d$	Lattice plane distance
$n$	Integer
$\theta$	Scattering angle
$\nu$	Frequency
$t$	Grain sizes
$I$	Intensity of beam
$A$	Absorbance
$\epsilon$	Molar absorptivity

C	Cell concentration
$\varepsilon_z$	Strain
$\sigma$	Stress
C	Elastic stiffness constants
G	Surface conductance
e	Electron
I	Current
V	Voltage

# **PERMUKAAN ZARAH ZnO YANG ROSAK DAN PENGARUHNYA TERHADAP SIFAT OPTIKAL, ELEKTRONIK DAN KETOKSIKAN**

## **ABSTRAK**

Kemoterapi, radiasi, dan pembedahan adalah rawatan yang paling biasa untuk kanser dalam beberapa tahun kebelakangan ini. Kanser adalah gangguan yang disebabkan oleh pembiakan sel malignan yang tidak terkawal. Walaupun secara teori semua rawatan ini sepatutnya berjaya memusnahkan sel-sel kanser, teknik terapeutik tidak selektif bagaimanapun membawa beberapa risiko utama. Penyelidikan baru-baru ini telah menunjukkan bahawa zink oksida (ZnO) berpotensi untuk mengatasi kesan sampingan ini disebabkan oleh biokompatibiliti yang tinggi, kemudahan kefungsi permukaan, keupayaan untuk menyasarkan kemaglinanan dan keupayaan angkutan ubat. Faedah ini membolehkan ZnO dipilih sebagai platform biokompatibel dan terbiodegradasikan, serta disiasat untuk rawatan kanser. Objektif utama kerja penyelidikan ini adalah untuk mengkaji kesan pengubahsuaian permukaan melalui persekitaran penyepuhlindapan yang berbeza terhadap sifat struktur ZnO dengan korelasi mereka terhadap sel barah payudara (MCF-7). Tiga sampel serbuk ZnO, (i) sampel tulen (ZnO-AG), (ii) penyepuhlindapan oksigen (ZnO-O<sub>2</sub>) dan (iii) sampel penyepuhlindapan nitrogen (ZnO-N<sub>2</sub>) dicirikan berdasarkan ciri morfologi, struktur, elektrik serta optic disiasat. Morfologi umum sampel ZnO terdiri daripada rod, plat, tripod, dan struktur seperti dram, serta bentuk yang tidak sekata. ZnO mempunyai diameter 30-200 nm manakala ketebalan 90-400 nm. Pengimejan elektron pengimbasan menunjukkan taburan oksigen dan atom zink (O: Zn) pada sampel ZnO di mana ZnO-O<sub>2</sub> mempunyai nisbah O: Zn yang lebih tinggi berbanding ZnO-N<sub>2</sub> pada permukaan ZnO. Pada suhu penyepuhlindapan 700°C, penyerapan oksigen tinggi berlaku pada permukaan ZnO-O<sub>2</sub> sementara penyerapan oksigen berlaku pada

permukaan ZnO-N<sub>2</sub>. ZnO-O<sub>2</sub> akan mengurangi kekonduksian permukaan sementara ZnO-N<sub>2</sub> meningkatkan kekonduksian permukaan. Pengukuran XRD menunjukkan sifat polihabluran yang sangat tinggi. Spektrum UV-Vis mendedahkan bahawa jurang jalur berkurangan dalam ZnO-O<sub>2</sub> dan ZnO-N<sub>2</sub>. Selain itu, puncak yang tinggi, E<sub>2</sub> (tinggi) diperoleh dari spektrum Raman. Pengukuran foto pendarcahaya mendedahkan ZnO-O<sub>2</sub> menunjukkan pelepasan hijau yang lebih rendah sementara ZnO-N<sub>2</sub> sebaliknya. Sementara itu, tindak balas kesitotoksian struktur ZnO dikaji terhadap sel fibroblas tikus L929 dan sel barah MCF-7. Sel L929 telah terdedah kepada semua sampel ZnO pada kepekatan 0.3125, 0.625, 1.25, 2.50, dan 5 mM selama 72 jam. Kepekatan di bawah 2.50 mM selamat untuk sel L929. Sel MCF-7 telah didedahkan kepada semua sampel ZnO pada kepekatan 0.1, 0.15, 0.18, 0.2 dan 0.25 mM selama 72 jam. Kepekatan perencatan separuh maksimum (IC<sub>50</sub>) untuk ZnO-AG dan ZnO-O<sub>2</sub> adalah 0.15 mM manakala ZnO-N<sub>2</sub> menunjukkan IC<sub>50</sub> sebanyak 0.18 mM. Kepekatan terbaik yang boleh digunakan ialah antara 0.1mM hingga 0.18 mM. Pembebasan ion zink dan penghasilan spesies oksigen reaktif (ROS) disarankan sebagai mekanisma ketoksikan yang berpotensi terhadap sel MCF-7. ZnO-O<sub>2</sub> dan ZnO-N<sub>2</sub> menunjukkan potensi tindak balas antikanser terhadap sel MCF-7.

# **DEFECTIVE PARTICLE SURFACE ON ZnO AND ITS INFLUENCE ON THE OPTICAL, ELECTRONIC AND TOXICITY PROPERTIES**

## **ABSTRACT**

Chemotherapy, radiation, and surgery are the most common treatments for cancer in recent years. Cancer is a disorder marked by uncontrolled malignant cell proliferation. Although in theory, all these treatments should be very successful at destroying cancer cells, nonselective therapeutic techniques nevertheless carry several major risks. Recent research has shown that zinc oxide (ZnO) has the potential to overcome these side effects due to its high biocompatibility, ease of surface functionalization, ability to target malignancy, and drug transport capability. These benefits allow ZnO to be chosen as biocompatible and biodegradable platforms, as well as being investigated for cancer treatment. The main objective of this study is to investigate how surface modification via various annealing ambient affects the properties of ZnO structures and how they relate to breast cancer cell survival (MCF-7). The morphological, structural, electrical, and optical properties of three ZnO (i) as grown (ZnO-AG), (ii) oxygen annealed (ZnO-O<sub>2</sub>) and (iii) nitrogen annealed (ZnO-N<sub>2</sub>) samples were investigated. The general morphologies of ZnO samples comprise rods, plates, tripod, and drumlike structures, as well as irregular shapes. The ZnO had a diameter of 30-200 nm while thickness 90-400 nm. Electron spectroscopy imaging (ESI) revealed oxygen and zinc atoms (O: Zn) distribution on the ZnO samples. On the ZnO surface, ZnO-O<sub>2</sub> had a greater O:Zn ratio while ZnO-N<sub>2</sub> had a lower O:Zn ratio. At 700°C, there was more oxygen adsorption on the ZnO-O<sub>2</sub> surface whereas there was more oxygen desorption on the ZnO-N<sub>2</sub> surface. Surface conductivity is reduced by ZnO-O<sub>2</sub>, whereas surface conductivity is increased by ZnO-N<sub>2</sub>. The highly polycrystalline properties of the ZnO sample were revealed by the XRD measurement.

The UV-Vis spectra discovered that the bandgap decreased in ZnO-O<sub>2</sub> and ZnO-N<sub>2</sub>. Besides, the Raman spectrum revealed an intense peak, E<sub>2</sub> (high). A photoluminescence study revealed ZnO-O<sub>2</sub> exhibited lower green emission than ZnO-N<sub>2</sub>. Meanwhile, cytotoxicity responses of ZnO structures were studied towards L929 cell lines and MCF-7 cancer cells. L929 cells were exposed to all ZnO samples at concentrations of 0.3125, 0.625, 1.25, 2.50, and 5 mM for 72 hours. The concentrations below 2.50 mM can be safe for L929 cells. MCF-7 cells were exposed to all ZnO samples at concentrations of 0.1, 0.15, 0.18, 0.2, and 0.25 mM for 72 hours. The half-maximal Inhibitory Concentration (IC<sub>50</sub>) was determined to be 0.15 mM for ZnO-AG and ZnO-O<sub>2</sub> while the ZnO-N<sub>2</sub> showed IC<sub>50</sub> of 0.18 mM. The best concentrations that can be used were between 0.1 mM and 0.18 mM. The zinc ions (Zn<sup>2+</sup>) released, and the generation of reactive oxygen species (ROS) has been proposed as potential toxicity mechanisms in the MCF-7 cell lines. ZnO-O<sub>2</sub> and ZnO-N<sub>2</sub> samples showed a potential for anticancer response towards MCF-7 cells.

# CHAPTER 1

## INTRODUCTION

### 1.1 Background of Study

Different morphologies of ZnO structures have been investigated for example rings, tubes, belts, wires, rods, plates, tetrapods, combs, and flowers with varying dimensions. Impurities and defects influence are dependent on a wide range of ZnO applications (Wang, 2004; Yahya et al., 2010). In addition, crystal orientation, particle size, morphology, oxygen defects and crystallinity are all key elements in influencing ZnO's optical, electrical, catalytic, and structural properties even the anti-cancer activity of ZnO. The large surface area of nano-scale structures, atomic arrangement even chemical compositions substantially modify their optoelectronic applications. To develop varied surface defects on the ZnO structure, annealing factors such as time, temperature, environment, and gas pressure can be changed.

An extensive study of the effects of annealing on ZnO thin films has been conducted. Several studies, on the other hand, yielded distinct experimental results. More investigation and explanation were needed on the optoelectronic and surface defect features of ZnO structures under various treatments. The production of defects, particularly oxygen vacancies, was connected to the presence of a nonstoichiometric chemical component in the samples. More research is needed to compare and assess the surface modification of oxygen and zinc ions concentrations after annealing ZnO powder samples with oxygen and nitrogen environments. The oxygen to zinc (O:Zn) ratio and surface band bending effect were recognized for the changes in the properties. In addition, surface defect and elemental distributions of ZnO were investigated using electron spectroscopy imaging (ESI).

Cell death was produced by ZnO with diverse structures that were manufactured utilising varied techniques, varying sizes, and selected concentrations. These structures were toxic to cells, anti-proliferative agents that might produce reactive oxygen species (ROS) and cause apoptosis. As a result, ZnO was recommended as a cancer-fighting agent (Akhtar et al., 2012; Premanathan et al., 2011). However, the specific mechanism of toxicity remains unknown, but some potential mechanisms have been described such as the generation of ROS (Guo et al., 2013), cell membrane disruption (Prach et al., 2013), and nanoparticles penetration into cells resulting in cell death (Nair et al., 2009; Wahab et al., 2013). The apoptosis induction has been identified as a causal factor in nanoparticles induced DNA damage (Meyer et al., 2011).

To investigate possible anti-cancer action, the nanosized ZnO shape, such as rods and plates with a higher surface-to-volume ratio, play a key role. Moreover, the anti-cancer properties of various structural morphologies vary. Further research into the cells' reaction to ZnO, as well as the driving mechanism, is needed due to the incidence and mortality of breast cancer are steadily growing. Even though many types of preventive and immunizations have been discovered, breast cancer still poses a serious threat to women's lives.

This study aims to investigate relationship between defect ZnO and human health, particularly cancer. The relationship between the ZnO's surface properties and the death of MCF-7 cancer cells was uncovered, and the mechanism of ZnO's anti-cancer effect has been proposed.



## 1.2 Problem Statement

In every country, cancer is a primary cause of death and a significant impediment to extending life expectancy. According to World Health Organization (WHO) estimates, cancer is the first or second major cause of death in 112 of 183 countries, and it ranks third or fourth in another 23 countries. Cancer continues to be one of the lethal diseases despite new medical innovations and technology developments (Mondal et al., 2020). The uncontrolled cell proliferation is one of the disease's hallmarks.

Cancer cells typically coexist with healthy cells and carry out their usual function in the body. The uncontrolled cell division results in excessive cell proliferation which caused cancer. The cancer cells are capable to develop their own blood supply, separate from the original organ, move and spread to additional body organs (Kim, 2015). The rise of cancer as a leading cause of death is partly due to significant reductions in the mortality rates of stroke and coronary heart disease in comparison to cancer in many nations (Sung et al., 2021). Hence, finding a cure for this deadly disease has become a top goal. The importance of physics in medicine, particularly in cancer treatment and diagnosis is well known.

Chemotherapy, radiation, and surgical techniques are the current methods employed to eliminate malignant cancer cells. However, there are still problems with postsurgical pain and complications, non-specific targeting and adverse effects of chemotherapy and radiotherapy (PDQ Adult Treatment Editorial Board, 2016). Besides that., these treatments' harmful side effects which kill both healthy body and damaged body cells are the main cause for concern (Liu et al., 2015). These treatments also have limitations as well such as low solubility, an inability to penetrate tumors

and considerable immune system and other organ damage. As a result, they have low survival rate (Mousa et al., 2011).

Zinc oxide (ZnO) is among the most widely used particle for drug delivery, cancer diagnostics and treatment due their unique physical and chemical properties. ZnO is employed in a range of industries including cosmetics, textile, electronics and being highly effective in the fight against cancer (Vasantharaj et al., 2021). ZnO also has a various application in medical since they are less toxic and more economical than other metal oxides. These applications include antibacterial, anti-aging, bioimaging and wound healing (Kim et al., 2017). ZnO has a high biocompatible which enables it to be used as antibacterial, antifungal and has potential as anticancer agent (Wiesmann et al., 2020). These results suggest that ZnO may be the ideal candidate for treating cancer.

Although ZnO has demonstrated remarkable potential in the detection and treatment of cancers, the development of safer alternatives, further improvements, more specific and thorough treatment approaches are needed including the use of ZnO nanoparticles that exhibit selective toxicity to specific breast cancer cells (Anjum et al., 2021).

The novelty of this work is the manipulation of ZnO surface properties by introducing physical defects on ZnO particles via oxygen/nitrogen annealing that generated different levels of Zn<sup>2+</sup> ions and ROS to efficiently kill breast cancer cell lines at low ZnO concentration.

### **1.3 Objectives of Study**

The main objectives of this research work are:

1. To characterize the ZnO structure due to structural, morphology and optoelectronic properties.
2. To investigate the surface modification effect on the ZnO properties structures using various annealing methods.
3. To study the anticancer effects of ZnO structures towards breast cancer line, (MCF-7).
4. To analyse the toxicity of ZnO structures on normal cell line (mouse skin fibroblast cell line L929).
5. To propose mechanism of ZnO toxicity towards MCF-7 cancer cells.

### **1.4 Scope of Study**

ZnO research covers a wide range of topics and investigations. The experimentation, results, and debates in this research endeavour are all guided by a definite and unambiguous scope. The scope of study consists of 3 main parts:

The first scope of this study is to investigate synthesized ZnO powder. In addition, the ZnO samples are made using the French method, which was used to create the majority of the ZnO powder consumed worldwide (Moezzi et al., 2012). Additionally, the analysis of different ZnO structures shows how this French technology is unique.

The second area of this research focuses on ZnO's anti-cancer activity against the MCF-7 cancer cell and cytotoxicity of the ZnO on normal cell (mouse skin fibroblast L929 cell line). This evaluation is extremely crucial caused by ZnO particles

are widely recognised for their toxicity towards target cancer cells while having less or no effect on other human normal cells. Following that, a variety of assays were carried out, including the determination of inhibitory concentrations ( $IC_{50}$ ), cell proliferation assay and microscopy observation of morphology changes. The responses of the L929 and MCF-7 cells were explored and correlated with ZnO characteristics as well as leading mechanisms involved such as toxicity of zinc and reactive oxygen species production.

The last study scope is to identify the morphology, optical, electrical and cytotoxicity properties of as grown ZnO (ZnO-AG) samples and ZnO annealed with oxygen, ZnO-O<sub>2</sub> and nitrogen, ZnO-N<sub>2</sub> using IV, XRD, FESEM-EDS, EFTEM-ESI, UV-Vis, PL and Raman properties of ZnO. Those were done to explain mechanism as result of the annealed ZnO towards on MCF-7 cells.

## **1.5 Thesis Outline**

Chapter 1 reviews the background study and the problem statements of the research. This chapter will also present the objectives and scopes of study. The thesis outline is also described.

Chapter 2 covers a literature review of physical, crystallinity, defect formation and energy levels of ZnO properties. Surface recombination, surface band bending, and lattice defects are given specific attention to explore the atomic organisation and crystalline orientation of ZnO formations. Besides, different annealing treatment (oxygen and nitrogen) on ZnO powder, reactive oxygen species (ROS), toxicity of ZnO nanoparticles, ZnO's activity on breast cancer line (MCF-7) and ZnO toxicity mechanism are all discussed.

Chapter 3 concentrates on sample preparations and methodologies for characterization employed using FESEM, EFTEM-ESI, XRD, PL, UV-Vis, Raman and IV were discussed. ZnO underwent tests for cytotoxicity and anti-cancer activity.

Chapter 4 provides descriptions of all experimental results between ZnO-AG, ZnO-O<sub>2</sub> and ZnO-N<sub>2</sub>. Additionally, the mechanisms and toxicity in anticancer activities of ZnO structures are explored.

Finally, Chapter 5 concludes the study. Future perspectives of this research are also presented.

## **CHAPTER 2**

### **LITERATURE REVIEW**

#### **2.1 Introduction**

Firstly, the applications of ZnO are described and physical, structural, electrical, and optical properties of ZnO are described. Then, type of annealing ambient on ZnO are discussed, followed by principles of the toxicity of ZnO towards cancer cell is presents briefly described in this chapter. The breast cancer is selected for anti-cancer study are addressed and explanation for mechanism of ZnO toxicity is clarified.

#### **2.2 Nanomaterial**

Nanotechnology is a cutting-edge field of study that enables for the creation of a diverse range of materials containing particulate elements of fewer than 100 nanometres (nm) in at least one dimension. Nanotechnology is the science of controlling the shape and size of structures at the nanoscale level in the design, characterization, manufacturing, and application of structures, devices, and systems. Aside from that, nanotechnology must deal with tiny things in a way that takes use of nanoscale-specific properties (Bayda et al., 2020).

Nanomaterials have risen to prominence as an intriguing new class of materials with a wide variety of practical uses. Nanomaterials are chemical compounds or materials that are created and utilised in at least one dimension at a very tiny scale between 1–100 nm (Ijaz et al., 2020).

The nanoparticles can be classified based on their dimensionality and divided into 4 classes as 0-dimensional (nanoparticles), 1-dimensional (nanorods, nanowires), 2-dimensional (nanofilms, nanolayers) and 3-dimensional (nanocrystalline) (Kabir et al., 2018). Nanomaterials are gaining tremendous attention due to their unique and considerably enhanced properties in chemical, physical, and mechanical when compared with their bulk materials (Saleh, 2020).

Their surface-to-volume ratio increases as particle size decreases, and their properties are governed by surface atoms rather than the bulk of the material for small enough feature sizes. Thus, due to their unique properties, nanomaterials have attracted considerable interest and constitute an increasingly significant material in the creation of novel nanotechnology with applications in a wide range of physical, biological, biomedical, and pharmaceutical applications (Khan et al., 2019). Nanomaterials are increasingly being used in drug delivery, chemical and biological sensing, gas sensing, solar cells, sunblock, cosmetics and antimicrobials (Shin et al., 2015).

Despite advancements in and future applications, the knowledge on the potential impacts of nanomaterials on human and environment health is still lacking. The environmental effects and toxicity of nanomaterials in terms of their interactions with biological components are remain unclear.

The increasing use of nanomaterials in commercial applications been questioned if the toxicity of nanomaterials poses any extra risks. Recognition on the potential of nanomaterials to the environment and human health is critically crucial to pursue their development in the future (Pattan et al., 2014).

### 2.3 ZnO Powder

Zinc occurs naturally as a metallic element, but it can be obtained in pure form only by smelting process. Zinc was initially discovered in India in the 14<sup>th</sup> century (Alam, 2020). It's a white powder that is almost insoluble in water. ZnO attracted much attention from researchers since it is produced synthetically for most commercial uses. ZnO attracted much attention from researchers since for most commercial uses, it is produced synthetically. During the 19<sup>th</sup> century, there are two large scale processes have been used for ZnO synthesis called indirect (French process) and direct (American process).

Until recently, the French process has produced the most amount of ZnO due to fastest and most dynamic method of generating ZnO (Buxbaum et al., 2005). LeClaire popularised the indirect technique in 1844, and it has been known as the French process ever since. Zinc metal is melted and evaporated at around 910 °C in the furnace (Mahmud et al., 2006).

Zinc oxide is formed when zinc vapour reacts with oxygen from the air. Zinc oxide particles are conveyed through a cooling duct and collected at a bag filter station. Agglomerates with an average particle size ranging from 0.1 to a few micrometres make up the product (Mahmud et al., 2006).

The ZnO particle shape are mainly nanorods, nanoplates, nanoboxes, nanomallets, microclusters, polyhedral drums and irregularly-shaped particles as showed in Figure 2.1 (Mahmud et al., 2006).



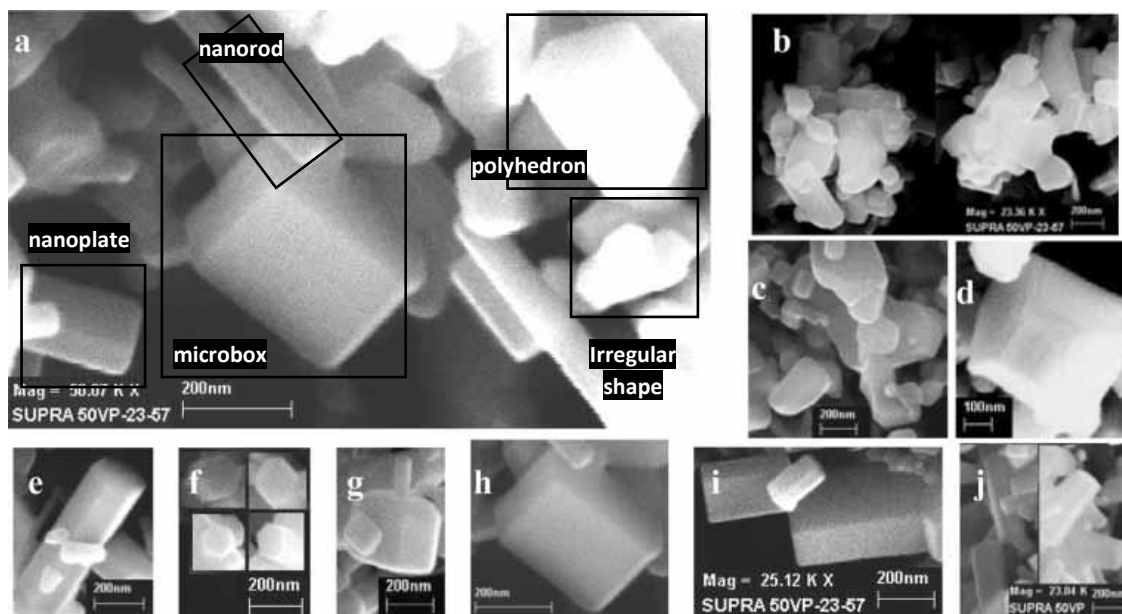


**Figure 2.1:** Shape of ZnO (a) five different nanostructures (microbox, nanorod, nanopl原因, polyhedron, ISP) (b) microclusters, (c) irregularly shaped particles (ISP) (d) hexagonal drum, (e) microrod, (f) hexagonal heads of nanorod, (g) nanomallet, (h) microbox, (i) family of nanoplates, (j) long rectangular nanoplates (Mahmud et al., 2006).

The powder ZnO is widely used in various products such as ceramics, glass, cement, rubber (e.g., car tyres), lubricants, paints, ointments, adhesives, plastics, sealants, pigments, foods (source of Zn nutrient), batteries, ferrites, and fire retardants (Sabir et al., 2014). The growing popularity of nano ZnO due to broad areas including technological development in the manufacture of ZnO nanostructures with novel physical properties that enable previously unknown applications and possibilities. Additionally, ZnO is easy to fabricate, environmentally friendly nature, and non-toxic synthesis route.

## 2.4 Application of ZnO

ZnO is presently widely used in a variety of fields, and it is classified as a promising, versatile functional and strategic material, owing to its broad range of uses. ZnO is being used as a constituent in more and more industries because of its unique

features. The multitudinous applications of ZnO NPs across a variety of fields such as optoelectronics, rubber industry, anticancer (Dhandapani et al., 2020), antibacterial (Dulta et al., 2021), drug delivery (Gavrilenko et al., 2020) and cosmetic (George et al., 2020) have been presented in Figure 2.2.

Due to the fundamental advantages such as direct wide bandgap, 3.37eV and higher exciton binding energy, ZnO based materials are viable candidates for numerous applications such as optoelectronics applications and sensor (Lee, 2010). Due to the lack of a centre of symmetry in ZnO's wurtzite structure, as well as significant electromechanical coupling effects, piezoelectric and pyroelectric capabilities can be exploited in piezoelectric sensors and mechanical actuators (Song et al., 2008; Wang et al., 2006)

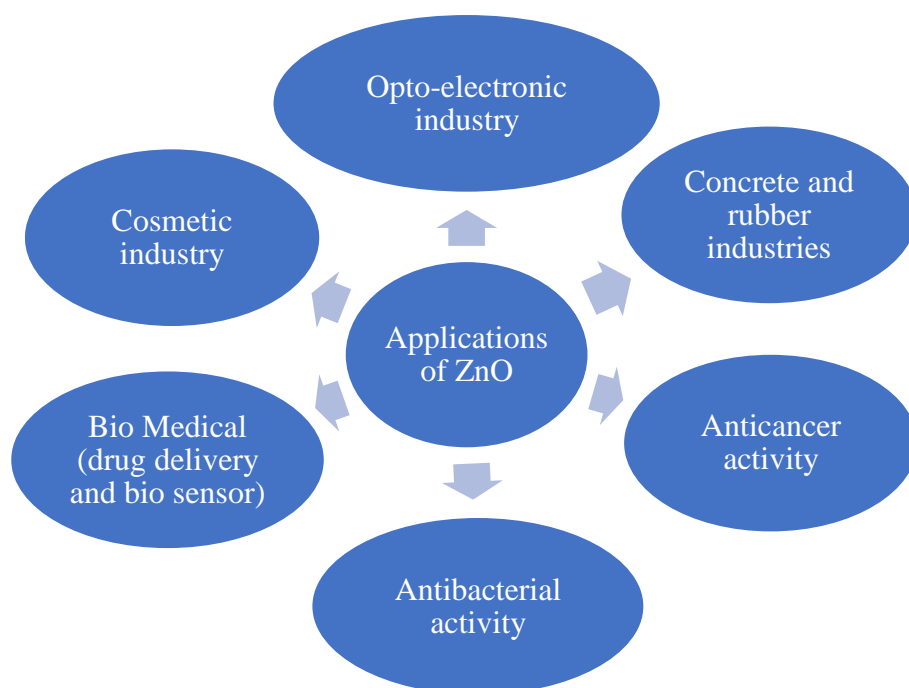


**Figure 2.2:** Applications of ZnO.

ZnO is a common additive used in the rubber industry. When applied, even in small concentrations, ZnO increases the heat conductivity of silicone rubber, just like a variety of other metal oxides and inorganic compounds do. It accomplishes this while keeping the silicone rubber's high electrical resistance (Raha et al., 2022).

Due to the implementation of nanotechnology, the biomedicine area in cancer field perceived a developed revolution. A growing number of studies have demonstrated the capacity of nanomaterials and specific metal oxide nanoparticles to kill cancer cells at low concentrations, while they have no impact on their micrometric counterparts. ZnO are one of these nanomaterials has made significant advances in biomedical applications for diagnostic as well as therapeutic. ZnO has demonstrated remarkable potential advancement in cancer treatment, such as its influence on human malignant lung cells and leukemia cancer cells (Tanino et al., 2020; Guo et al., 2008).

ZnO has excellent antibacterial capabilities, including a strong ability to inhibit pathogenic pathogens and a high surface reactive area. ZnO has the capacity to drive the production of excessive reactive oxygen species, including hydroxyl radicals, superoxide anion, and hydrogen peroxide, as well as an antibacterial toxicity mechanism (Vassallo et al., 2020).

ZnO has potential for drug delivery in a range of diseases. ZnO encapsulated with chitosan, carrying improved stability, were efficient for importing doxorubicin (DOX) into cancer cells. ZnO was successfully exploited as delivery systems for both gene transport and gene silencing (Raha et al., 2022).

ZnO is frequently employed in the production of many raw materials used in medicine, such as disinfection agents and for dermatological applications, due to its antibacterial and effective antifungal activity. UVA and UVB radiations are absorbed by ZnO, which can be found in sunblock (Singh, 2013).

## 2.5 Properties of ZnO

ZnO is a binary semiconductor belonging to the II-VI compound that melts around 1975 °C. ZnO crystallises as wurtzite at room temperature, a hexagonal close-packed sub-lattice with the anion (oxygen) and cation (zinc) displaced in the [0001] direction. It has a hexagonal unit cell that belongs to P63mc space group  $C_{6v}^4$ . Each zinc atom in the wurtzite lattice is connected to four oxygen atoms in a tetrahedron's vertices via  $sp^3$  covalent bonding (Özgür et al., 2005).

In bulk ZnO, the Zn-O link has both covalent and ionic properties. The Zn-O bond has a Wiberg index  $W$  (ZnO) of 0.11e, a zinc valence of 0.47, and a total quantum chemical valence of 2.0 (Ermoshin et al. 1995). A wurtzite lattice's axes and faces are indicated by the four-digit Miller indices  $hkil$ . The hexagonal (0001) plane is perpendicular to the  $c$ -axis, and the  $c$ -axis direction is referred to as [0001] plane.

A schematic presentation of the wurtzite ZnO structure is shown in Figure 2.3. The three parameters of the wurtzite lattice for a hexagonal unit cell are the internal coordinate,  $u=3/8= 0.375$ , the uniaxial lattice constant,  $c=5.2069$ , and the basal plane lattice constant,  $a=3.2495$  (Morkoç et al., 2009). Furthermore, the basal plane is the most prevalent polar surface on ZnO. Several properties of zinc oxide are listed in Table 2.1 (Fan et al., 2005).

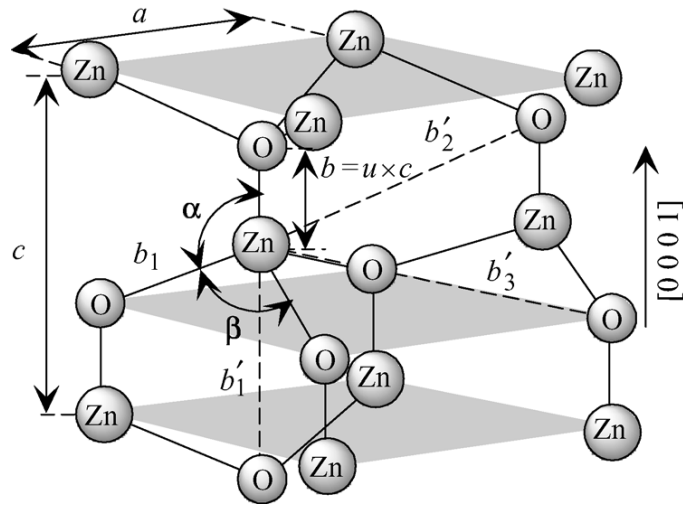


**Figure 2.3:** Hexagonal wurtzite-type lattice of ZnO crystal structure (Morkoç et al., 2009).

**Table 2.1:** Typical properties of ZnO.

Properties	Values
Lattice constant (T=27 °C)	$a_0 = 0.32469$ nm $c_0 = 0.52069$ nm
Density	5.6066 g/ cm <sup>3</sup>
Molecular mass	81.389 g/ mol
Melting point	1975 °C
Electron effective mass	0.24 $m_0$
Hole effective mass	0.59 $m_0$
Relative dielectric constant	8.66
Refractive index	2.004
Bandgap energy at 27 °C	3.37 eV
Exciton binding energy	60 meV
Thermal conductivity	0.6 – 1.2 Wcm <sup>-1</sup> °C <sup>-1</sup>
Specific heat capacity at constant pressure, $C_p$	9.62 calmol <sup>-1</sup> °C <sup>-1</sup>
Electron mobility (T=27 °C)	200 cm <sup>2</sup> / Vs

## 2.6 Electrical Properties of ZnO

ZnO is a semiconductor with a huge and direct bandgap that attracts a lot of interest in optoelectronic applications. High-power and high-temperature operations, lesser noise production, ability to endure huge electric fields, and higher breakdown voltages are the advantages of having a large bandgap (Millán et al., 2012). ZnO attracts a lot of interest for optoelectronic device applications due to the exciton binding energy of 60 meV at 27 °C. The effective mass of electron is  $0.24 m_0$ , and the effective mass of hole is  $0.59 m_0$  (Fan et al 2005).

A wurtzite phase of as grown ZnO is n-type by nature due to stoichiometry deviations caused by intrinsic defects like zinc interstitials ( $Zn_i$ ), antisites and oxygen vacancies ( $V_o$ ) that developed during growth. Obtaining p-type doping remain a question. While some researcher have reported obtaining p-type ZnO, there are still concerns about the results' reproducibility and the p-type conductivity's stability (Janotti et al., 2009).

During growth or annealing, the conductivity of ZnO is also heavily influenced by stoichiometry, oxygen, or zinc partial pressure. The electrical carrier concentration and conductivity of the crystals were modified by annealing at varied oxygen partial pressures due to the reaction between oxygen vacancies or interstitial zinc atoms and electrons in the conduction band. (Tomlins et al., 2000) investigated the self-diffusion and electrical transport characteristics of zinc in ZnO single crystals. Zinc diffusion was most likely governed by a vacancy mechanism. The n-type conductivity of ZnO was induced by oxygen vacancies (Tomlins et al., 2000). The ZnO diffusion constants and defect generation energies, where oxygen vacancies and zinc interstitials function

as energetic shallow donor sites in the band gap, while zinc interstitials and oxygen vacancies function as acceptors (Erhart et al., 2006).

## **2.7 Optical Properties of ZnO**

The optical properties of a semiconductor are influenced by both internal and external imperfections. Between electrons in the conduction band and holes in the valence band, intrinsic optical transitions occur. On the other hand, extrinsic characteristics are related to dopants, point defects, and complexes, which manage producing electronic states in the bandgap. Both optical absorption and emission processes can be impacted by impurities.

Lattice dynamics and energy band structure have an impact on the optical properties and electronic states of bound excitons in ZnO. The laser emission from ZnO-based devices operating at 27 °C with small threshold currents had been demonstrated by several groups (Meyer et al., 2004). MgO or CdO alloyed can changed the band gap energy of ZnO to higher or lower value (Choopun et al., 2002). Additionally, doping ZnO with Al or Ga allows for the monitoring of its n-type electrical conductivity (Minami, 2000).

In Raman spectra of ZnO nanostructures, two plausible causes for phonon peak shifts have been identified. The spatial confinement within the nanocrystal or quantum dot limits is the first reason. Second, imperfections such as oxygen vacancies, zinc excess, surface contaminants, and other defects are linked to phonon localization. The defects in nano-sized crystals or quantum dots produced using chemical methods or molecular-beam evaporation are often greater than those in bulk crystals.

The Raman spectra of nanocrystalline semiconductors are redshifted and widened due to the relaxing of the phonon wave vector due to the limited size nanocrystals, according to the optical phonon's spatial confinement. Because of the optical anisotropy of the wurtzite lattice, optical-phonon confinement in wurtzite nanocrystals causes minor alterations in Raman spectra (Fonoberov et al., 2006).

Standard ZnO generally exhibits two different types of emissions in its photoluminescence (PL) spectrum at room temperature which are a broad visible and a UV emission band. Deep level emission (DLE) is a broad visible emission band with a wavelength of between 420 and 700 nm, whereas UV emission is related to either excitonic recombination or a band-edge transition of ZnO. Many investigations have been done on the DLE's origin. Oxygen vacancies ( $V_o$ ), zinc vacancies ( $V_{Zn}$ ), oxygen interstitials ( $O_i$ ), and zinc interstitials ( $Zn_i$ ) are some structural defects that have been associated with the DLE band (Yamauchi et al., 2004).

In semiconductors, there are two types of recombination mechanisms. The first one is radiative recombination. In this recombination, a photon with an energy equivalent to or close to the semiconductor's bandgap energy was released, as shown in Figure 2.4. Photon emission from direct bandgap ZnO was caused by the recombination of a free electron with a hole (Schubert, 2006).

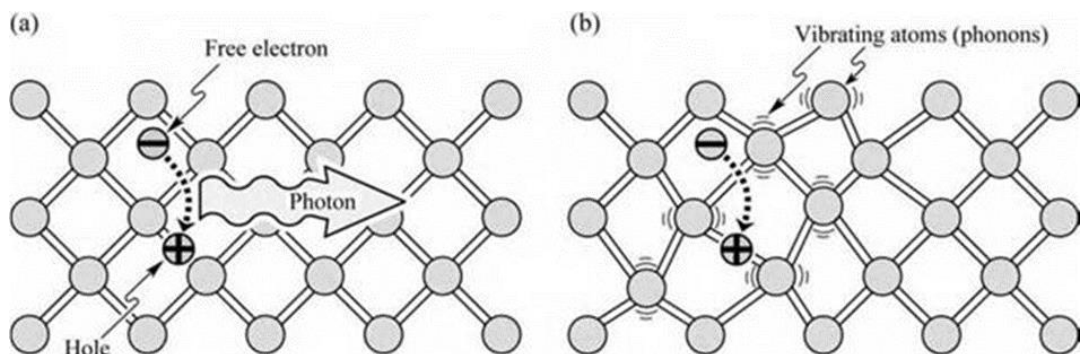


**Figure 2.4:** (a) Radiative recombination; (b) non-radiative recombination (Schubert, 2006).



The electron energy is converted to the vibrational energy of the lattice atoms, or phonons, during non-radiative recombination. Heat is produced because of the conversion of electron energy to heat. Nonradiative recombination events in light-emitting devices are undesirable for obvious reasons. There are three types of non-radiative recombination. The first one is non-radiative through deep level energy transition. Second is Auger recombination, and the last one is surface recombination. Figure 2.5 depicts non-radiative mechanisms such as deep level energy transitions and Auger recombination.

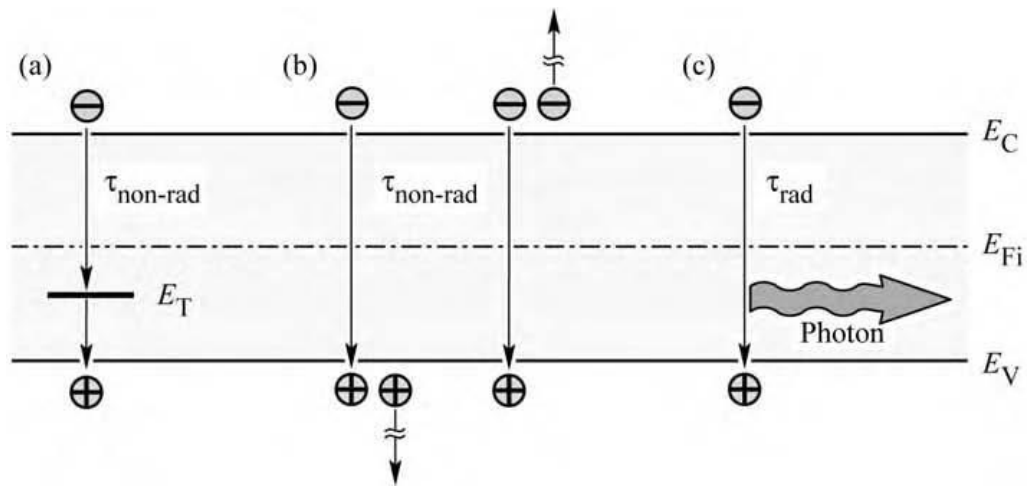


**Figure 2.5:** Band transitions in a semiconductor (a) non-radiative via deep level (b) non-radiative via Auger process (c) radiative with a photon emission (Schubert, 2006).

### 2.7.1 Non-radiative Via Deep Level Energy

Non-radiative recombination is caused by crystallographic defect like dislocations, impurities, native defects, and other complexes of defects. The semiconductor's forbidden gap is filled by one or more energy levels created by native defects, such as interstitials, vacancies, and antisite defects. Figure 2.6 displays the projected defect energy levels for ZnO based on several literature sources.

The acceptor defects are  $V_{zn}''$ ,  $V_{zn}'$  and the donor defects are  $Zn_i^{\cdot\cdot}$ ,  $Zn_i^{\cdot}$ ,  $Zn_i^{\times}$ ,  $V_o^{\cdot\cdot}$ ,  $V_o^{\cdot}$ ,  $V_o^{\times}$ . Radiative or non-radiative recombination occurs at this level. Energy level generates recombination centres within the semiconductor gap, which operate as shallow or deep level energy. Deep levels in the semiconductor's forbidden energy gap operate like carrier recombination or trapping centres, reducing device performance. Energy level generates recombination centres within the semiconductor gap, which operate as shallow or deep level energy. Deep levels in the semiconductor's forbidden energy gap operate as carrier recombination or trapping centres, reducing device performance. Deep levels in semiconductor can be caused by native defects in the lattice (Oba et al., 2010).

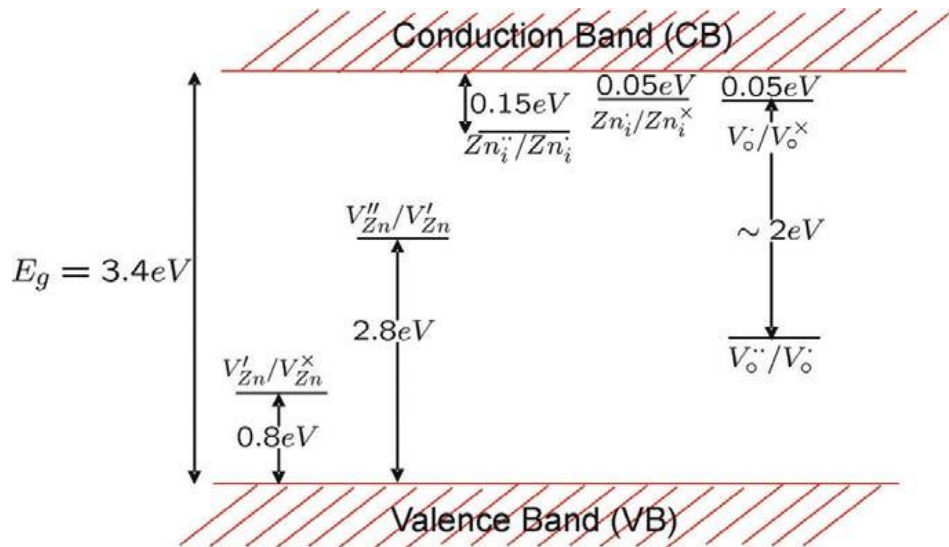


**Figure 2.6:** Energy levels of native defects in ZnO (Schmidt-Mende et., 2007).

### 2.7.2 Auger Recombination

In direct bandgap materials, the Auger recombination mechanism, as showed in Figure 2.7, is significant. A non-radiative kind of recombination is auger recombination. Auger recombination can occur in two ways. The first one is recombination of a hole and an electron that results in energy transfer to another free hole. The second one is recombination of a hole and an electron that results in energy

transfer to a free electron. A third carrier receives the energy and is excited to a higher energy level without switching to a different frequency band. Thermal vibrations will then lose the third carrier's excess energy (Schubert, 2006).

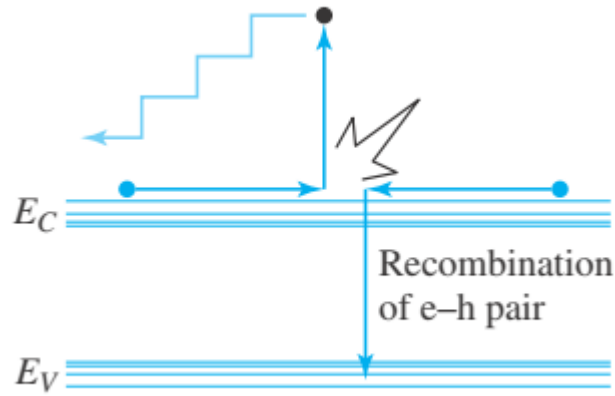


**Figure 2.7:** The Auger recombination process (Dimitrijević, 2012).

### 2.7.3 Surface recombination

Semiconductor surfaces are often made up of dangling bonds, electronically active and unsaturated interatomic bond at the surface of semiconductor. They allow many defects to form on the surface, resulting in a dispersion of defect states in the surface band gap. The total charge state at the surface, as depicted in Figure 2.8, serves as the anchor for the Fermi level. There is more recombination at the surface due to the high density of these surface states. For an extrinsic n-type semiconductor, the relation may be used to calculate the recombination rate of surplus carriers,  $R_s$  in the bulk as Equation 2.1:

$$R_s = \frac{\delta p_s}{\tau_{p0s}} \quad (2.1)$$

Where  $\delta p_s$  is the concentration of excess mobility carrier holes at the surface, and  $\tau_{p0s}$  is the lifetime of excess minority carrier holes at the surface. Surface recombination can be decreased by creating a heterojunction at the free surface or

adding a dielectric ( $\text{SiO}_2$  or  $\text{Si}_3\text{N}_4$ ). To tie up certain hanging links, an additional layer is produced on top of the films. Surface recombination was achieved using thermal post-annealing or enhanced growth pressure in ZnO-NS, which was produced in chemical solutions (Oba et al., 2010).

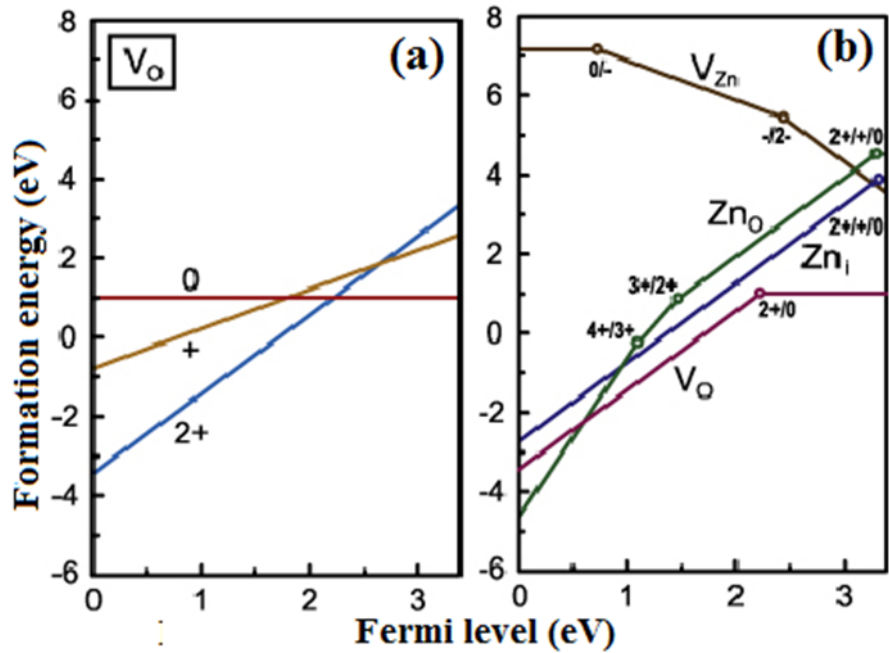


**Figure 2.8:** Fermi level is pinned by the overall charge state at the surface (a) formation energies of the O vacancy ( $V_O$ ) (b) formation energies of  $V_O$ , the Zn interstitial ( $Zn_i$ ), the Zn antisite ( $ZnO$ ), and the Zn vacancy ( $V_{Zn}$ ) (Oba et al., 2010).

## 2.8 Surface Modification of ZnO by Annealing

Researchers have been experimenting with numerous strategies to modify the surfaces of molecules in recent years. The key to effective nanomaterial applications is to optimise their surface physical and chemical characteristics. Thermal annealing is a commonly used method for improving crystal quality, which improves optical, structural, and electrical properties by reducing material defects. ZnO's surface quality could be improved by annealing, a technique that removes surface imperfections and contaminants (Byrne et al., 2010; Maffei et al., 2012). Although the effect of annealing temperature of the performance of the UV photoconductive sensor has

widely reported, the effects of annealing under different ambient have hardly been described in terms of the performance of ZnO nanorod-array-based UV photoconductive sensors (Kim et al., 2011; Zhou et al., 2011).

The modification of ZnO surfaces by annealing produce the best antibacterial responses (Sirelkhatim et al., 2015). The inhibition of ZnO powder can be significantly increased by annealing it. It was found by the researchers that oxygen annealing enhanced the quantity of oxygen atoms on the surface of ZnO samples, improving antibacterial response by increasing the amount of ROS in the suspension, causing significant oxidative stress on the bacteria. The release of  $Zn^{2+}$  ions and increased ROS generation might be achieved by altering the surface area of ZnO.

Mamat et al. (2012) increased the surface area of ZnO nanorods by annealed in oxygen and air to encourage the nanoholes formed on the surface, which resulted in high oxygen absorption and diffusion onto the surface during UV light exposure, assisting in the generation of more ROS on the surface.

Annealed ZnO has been discovered to play a crucial role in cancer therapy and diagnostics. Despite the wide applications of ZnO in the biomedical field, various limitation such as increased toxicity, has limits its clinical use. As a result, it's become critical to adjust nano scaled-ZnO surfaces so that they might profit from their core attractive and unique qualities while also improving their surface properties, resulting in efficient therapeutic formulations with minimal or no harmful effect on normal cells.

Another advantage of this modification is that any negative effects seen during treatment will be reduced or eliminated. The influence on their cytotoxicity capabilities, which is the main objective of modifying the surface, is the most significant alteration in the changed ZnO due to the well dispersed nanoparticles.

## 2.9 Toxicity of ZnO

Nanomaterials with a diameter of at least 100 nm are widely utilised in textiles, food additives, electronics, sunscreens, and cosmetics. This size range of materials may be approaching the length scale at which certain physical or chemical interactions with their surroundings can occur. As a result, their properties vary significantly from those of bulk materials of similar composition. This allowed them to achieve extraordinary reactivity, conductivity, and optical sensitivity. These capabilities may have unfavourable consequences, such as harmful interactions between the environment and biological system, which lead to generate toxicity. The establishment of principles and test procedures to ensure safe manufacture and use of nanomaterials in the marketplace is urgently required and achievable (Nel et al., 2006).

There is a significant number of literatures on metal oxide nanotoxicity in vitro models. Several research groups have investigated ZnO in particular and found that they exhibit different toxicological profiles in vitro than bulk ZnO (Nair et al., 2009; Wahab et al., 2010). Several adverse effects of ZnO-NPs have been explored in vitro (Lin et al., 2009; Yang et al., 2009) and in vivo (Wang et al., 2010; Xia et al., 2011), due to the rising interest in their potential toxicity to cells and bacterial. As a result, it is critical to examine the toxicity of nanoparticles prior to their application.

ZnO unique qualities allowed them to be used in a variety of products, including anti-dandruff shampoos, baby powders, welding fumes, sunscreen, and UV fabric treatments (Becheri et al., 2008; Wesselkamper et al., 2001). Furthermore, ZnO has emerged as a potential material for medical uses, such as anti-cancer characteristics and medication delivery (Akhtar et al., 2012).